Biomed Microdevices
DOI 10.1007/s10544-014-9842-8

Microfluidic direct writer with integrated declogging mechanism for fabricating cell-laden hydrogel constructs

Setareh Ghorbanian · Mohammad A. Qasaimeh · Mohsen Akbari · Ali Tamayol · David Juncker

Abstract Cell distribution and nutrient supply in 3D cell-laden hydrogel scaffolds are critical and should mimic the *in vivo* cellular environment, but been difficult to control with conventional fabrication methods. Here, we present a microfluidic direct writer (MFDW) to construct 3D cell-laden hydrogel structures with openings permitting media exchange. The MFDW comprises a monolithic microfluidic head, which delivers coaxial streams of cell-laden sodium alginate and calcium chloride solutions to form hydrogel fibers. Fiber diameter is controlled by adjusting the ratio of the volumetric flow rates. The MFDW head is mounted on a motorized stage, which is automatically controlled and moves at a speed synchronized with the speed of fiber fabrication. Head geometry, flow rates, and viscosity of the writing solutions were optimized to prevent the occurrence of curling and bulging. For continuous use, a highly reliable process is needed, which was accomplished with the integration of a declogging conduit supplying a solvent to dissolve the clogging gel. The MFDW was used for layer-by-layer fabrication of simple 3D structures with encapsulated cells. Assembly of 3D structures with distinct fibers is demonstrated by alternatively delivering two different alginate gel solutions. The MFDW head can be built rapidly and easily, and will allow 3D constructs for tissue engineering to be fabricated with multiple hydrogels and cell types.

Keywords Microfluidic coaxial flow · Direct writing · Cell-laden constructs · Calcium alginate · Tissue engineering · 3D cell scaffold

1 Introduction

It is now widely recognized that 3D cell cultures better replicate the *in vivo* cellular environment than conventional 2D cultures (Pampaloni et al. 2007; Yamada and Cukierman 2007). Creating a multicellular 3D environment, containing extracellular matrix (ECM) similar to the physiological environment, can therefore provide an environment that promotes regular cell adhesion, proliferation, and activities (Mazzoleni et al. 2009; Annabi et al. 2014). 3D cultures are used as a substitute to animal models for research in drug response and diagnostic research as they are cheaper, more reproducible and easier to control (Norotte et al. 2009; Shi et al. 2009). To accurately reproduce *in vivo* structures, different cells need to be distributed in the scaffold and a vascular network is required to transport nutrients and oxygen and remove metabolic waste. However, some classical scaffold fabrication methods, such as self-assembly, (Lutolf and Hubbell 2005) emulsion freeze-drying, (Ho et al. 2004) gas foaming (Harris et al. 1998; Wang et al. 2006; Chung et al. 2011), solvent casting and particle leaching (Nam and Park 1999; Vogelaar et al. 2003; Katoh et al. 2004; Tan et al. 2005; Park et al. 2007; Wiria et al. 2007), electrospinning (Yokoyama et al. 2009), and textile engineering (Moutos et al. 2007; Ellä et al. 2012) could not address all those requirements. Indeed, these methods either require harsh chemicals that are incompatible with biological entities, or cannot control their distribution. Moreover, the

Electronic supplementary material The online version of this article (doi:10.1007/s10544-014-9842-8) contains supplementary material, which is available to authorized users.

S. Ghorbanian · M. Akbari · A. Tamayol · D. Juncker (✉)
Biomedical Engineering Department, McGill University and Genome Quebec Innovation Centre, McGill University, Montréal, Canada
e-mail: david.juncker@mcgill.ca

M. A. Qasaimeh
Division of Engineering, New York University Abu Dhabi, Abu Dhabi, United Arab Emirates

D. Juncker
Department of Neurology and Neurosurgery, McGill University, Montréal, Quebec H3A 0G1, Canada

Published online: 04 March 2014

integration of interconnected pores similar to a vascular network is not feasible using the abovementioned methods.

Recently, computer aided bioprinting has emerged as a powerful tool for production of scaffolds and tissue constructs with high resolution and control over pore distribution, shape, and microstructure (Hollister 2005; Moroni et al. 2008; Gauvin et al. 2012) Bioprinting enables programmable delivery of scaffold materials, living cells, and growth factors at precise locations and quantities using commercial inkjet nozzles (Onoe et al. 2013; Annabi et al. 2014). In a more advanced implementation, cell-laden beads were printed and let to fuse together to form even structures and enhance the throughput (Fedorovich et al. 2012). A variety of synthetic and natural polymers can be used for direct printing of complex 3D structures for various applications such as bone (Landers et al. 2002; Kim et al. 2011; Lee et al. 2011b), cartilage (Neves et al. 2011; Fedorovich et al. 2012), and cardiac tissue engineering (Berry et al. 2011; Gaetani et al. 2012). The utilization of bioprinters in tissue engineering, however, faces several challenges. Bioprinters require sophisticated, miniaturized nozzles operating at high pressures, which can be harmful to cells, and that are prone to clogging.

Microfluidic devices have been adapted to produce beads and fibers with sizes between a few tens to a few hundred micrometers (Kang et al. 2011; Chung et al. 2012). For example, coaxial core-sheath streams of a prepolymer and a crosslinking solution, respectively, have been used for fabrication of hydrogel fibers using various materials such as alginate (Shin et al. 2007; Arumuganathar et al. 2008; Mazzitelli et al. 2011; Yamada et al. 2012), chitosan, poly(lactic-co-glycolic acid) (PLGA) (Hwang et al. 2008, 2009), and chitosan/alginate mixtures (Lee et al. 2011a). These fibers can in turn be assembled to form scaffolds using techniques derived from the textile industry such as rolling and weaving (Moutos et al. 2007; Onoe et al. 2013; Tamayol. et al 2013). However, these methods still face challenges such as handling fragile and wet hydrogel fibers. In a notable recent study, Leng et al. reported a microfluidic system for one-step formation of mosaic hydrogels on a biocompatible polymeric sheet (Leng et al. 2012). An array of microfluidic nozzles stacked into 10 layers continuously delivered hydrogel precursors that were extruded into sheets and maintained in place by a surrounding stream. The hydrogel sheets were crosslinked outside of the microfluidic nozzle and collected on a motorized roller. The mosaic hydrogel sheets were between 130 and 350 μm thick, 3 mm wide, and produced at a rapid rate of 10 mm/s. Patterning of the sheets was achieved by computer controlled elastomeric on/off valves, thus forming two dimensional patterns, but manual assembly was required for forming complex and arbitrary 3D constructs.

Here, we report a microfluidic direct writer (MFDW) that integrates the concepts of direct writing and microfluidic fiber spinning to create 3D cell-laden hydrogel constructs for the first time. Even though coaxial flow, within microfluidics devices, has previously been shown, they have not been used for direct writing, which we achieve and present in this work. Proposed MFDW enables the formation of 3D open porous structures with control over fiber diameter, pore size, and pore distribution. With this platform, process-induced mechanical damages to cells that may be caused due to the dispensing pressure and nozzle size can be minimized. In this work, we create calcium alginate fibers in a coaxial flow format with sodium alginate/cells as the core stream and calcium chloride ($CaCl_2$) as the sheath stream (Fig. 1). Cell-laden hydrogel fibers are deposited layer-by-layer on a substrate using an automated microscope stage until the final construct is formed. We designed a chemical declogging mechanism that allows on-site removal of hydrogel blockages and permits rapid resumption of direct writing. This mechanism is of great practical importance because once the alginate clogs within the MFDW, the removal of the gelled alginate might require the disassembly of the setup and starting anew. Hence, this added mechanism allows for rapid declogging and resumption of the ongoing writing process. The optimization of the microfluidic head, writing "inks", substrate, method for cell encapsulation to ensure cell survival, and overall setup for efficient fiber deposition are described.

2 Experimental

2.1 Materials

Sodium alginate, $CaCl_2$, ethylenediaminetetraacetic acid (EDTA), 3-aminopropyl-triethoxysilane 99 %, and trypan blue were purchased from Sigma Aldrich (St. Louis, MO, USA). Polydimethylsiloxane (PDMS, Sylgard 184) was obtained from Dow Corning (Midland, MI USA). Dulbecco's modified Eagle medium (DMEM), fetal bovine serum (FBS), 0.05 % trypsin-EDTA (1X), and antibiotics (penicillin/streptomycin) were purchased from Invitrogen (Burlington, ON, Canada). Cell growth medium was prepared by supplementing a DMEM medium with 10 % FBS and 1 % (v/v) antibiotics (final concentrations of 100 I.U./mL Penicillin and 100 (μg/mL) Streptomycin). A live/dead cell vitality Assay Kit (L34951) with C12 resazurin & SYTOX® Green were purchased from Invitrogen (Burlington, ON, Canada).

Sodium alginate was dissolved in distilled water, with a concentration of 2 % (w/v). The solution was stirred overnight at 40 °C, stored at 4 °C, and used for experiments for up to 2 months.

For cell experiments, cells in media were mixed with 2 % alginate 50:50 to make a final 1 % alginate solution. $CaCl_2$ solution was prepared by adding 50 ml glycerol to 50 ml of HEPES buffer (pH 7) and the subsequent addition of 2 g of $CaCl_2$ to form a 2 % (w/v) solution. The chelating solution was prepared from 30 mM EDTA and 0.15 M sodium chloride (NaCl) in 1 mM HEPES buffer and stored at 4 °C.

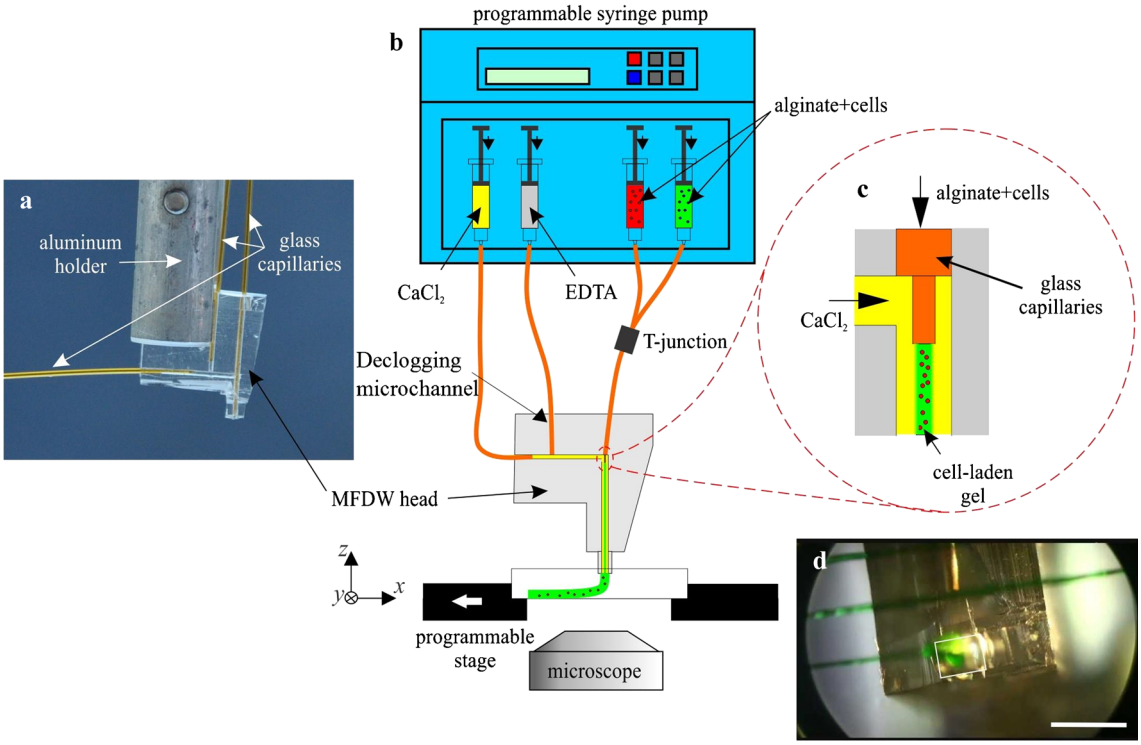

Fig. 1 Microfluidic direct writer (MFDW) setup, along with its key elements. The central image shows the MFDW during delivery of a fiber onto a substrate placed on a programmable XY stage, and the objective of an inverted microscope equipped with a CCD camera for direct observation. **a** Image of a MFDW head made of PDMS and Aluminum (Al) holder, along with capillaries used to connect it to the syringe pumps. The Al holder is connected to an XYZ micropositioner (not shown). **b** Schematic of the syringe pumps and capillaries for delivering two distinct alginate solutions mixed with cells, a $CaCl_2$ solution, and an EDTA solution injected only when clogging occurs (when the injection of alginate and $CaCl_2$ are stopped) to dissolve the hydrogel clogging the channel (see Fig. S1 for more details). **c** Close-up schematic of the flow sheathing achieved by inserting a smaller, central capillary within a larger, outer capillary, which in turn is inserted into the PDMS MFDW head. During the fiber formation process, $CaCl_2$ diffuses into the alginate solution and forms cell-laden fibers that are delivered through the head. **d** MFDW in the process of fiber patterning as observed with the inverted microscope. Green food dye was added to the alginate solution for visualization. Scale bar is 1.5 mm

All solutions were initially sterile filtered using a 0.22 μm filter and degassed by using a vacuum desiccator to remove bubbles. All syringes and capillaries were initially sterilized and rendered hydrophilic by rinsing with a 70 % ethanol solution, followed by phosphate buffered saline (PBS). Afterwards, syringes were filled with reagents and connected to capillaries with NanoTight™ connectors purchased from Upchurch Scientific (Oak Harbor, WA), Fig. S1.

Standard size microscope glass slides (50×75 mm^2), obtained from Corning (Corning, NY), were initially cleaned in acetone and ethanol with sonication, dried, and silanized by vapor deposition of 3-aminopropyl-triethoxysilane 99 %. Prior to each experiment, glass slides were sterilized under UV light for 30 min.

2.2 MFDW head fabrication and operation

A simple and cost-effective molding technique using glass capillaries was employed to fabricate the MFDW head with interconnected circular cross-section channels (Ghorbanian et al. 2010). Briefly, glass capillaries were cut to size, then arranged on a flat PDMS surface according to the desired architecture and covered with a second layer of PDMS, which was then cured. The size of each channel can be adjusted by selecting a capillary with the desired outer diameter, and different branch architectures can be produced by arranging the capillaries according to the desired configuration. Small gaps often remain at the junction of manually placed capillaries. To fill any residual gap, a small flake of paraffin was placed on top of each junction and melted prior to pouring the PDMS pre-polymer. After curing the PDMS, capillaries were removed from the slab, leaving behind a network of channels. The MFDW was then cut to the desired shape using a razor blade. The tip of the MFDW is critical, usually cut to less than 1 mm, to reduce the effect of the probe movement on flow disturbances, which can break the scaffold before its fully crosslinked. Also, a smaller tip allows placing fibers in close proximity of each other and hence improves the writing resolution.

The experimental setup of the MFDW (Fig. 2) is similar to the station used for operating microfluidic probes (Perrault

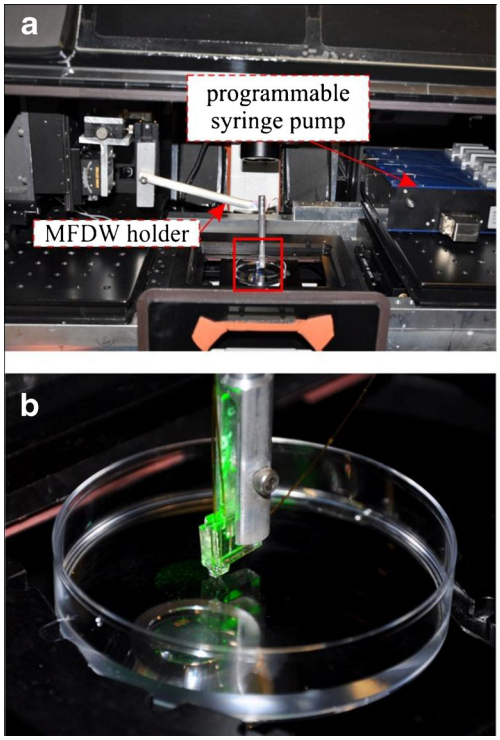

Fig. 2 The MFDW setup. **a** The setup comprises the MFDW head, a programmable stage, an XYZ micropositioner, an inverted microscope along with a CCD camera (not shown), capillaries (not visible), and syringe pumps. **b** A close-up view of the MFDW head

et al. 2010). Briefly, the MFDW head was secured with a clamping rod and mounted on an XYZ micro positioner (7600-XYZL, Siskiyou, Grants Pass, OR). The outlet of the MFDW head was positioned in close proximity to the transparent substrate (glass slide) on the automated microscope stage (PZ-2000, Applied Scientific Instrumentation, Eugene, OR) of an inverted microscope (TE2000, Nikon, Saint-Laurent, QC, Canada). Glass capillaries (Polymicro Technologies, Phoenix, AZ) were plugged into the MFDW head's inlets and connected to glass syringes (Hamilton, Reno, NV), which were operated using computer-controlled syringe pumps (Nemesys Cetoni, Korbussen, Germany).

2.3 Declogging mechanism

A declogging microchannel was added to deliver Ethylenediaminetetraacetic acid (EDTA), a Ca^{2+}chelator that was used to dissolve alginate gel blocking the outlet channel. The EDTA shares a common microchannel with the $CaCl_2$ (Fig. 1). Since alginate is initially crosslinked due to the presence of calcium, the removal of calcium by EDTA leads to the alginate getting dissolved. Upon observation of blockage within the MFDW head, all other pumps were stopped, then EDTA was delivered to the conduit to dissolve the solid gel. Once the clogged gel was removed, the writing process was resumed. In some cases, when clogging was large, the MFDW head was moved to another dish and more EDTA was injected until the clogging was resolved.

2.4 Image acquisition and analysis

Bright-field and fluorescent images were acquired using a cooled CCD camera (Photometrics CoolSNAP HQ2), connected to an inverted microscope. ImageJ 1.42 software (National Institutes of Health, Maryland) was used offline to analyze and color the acquired black and white images. Images of live and dead cells represented by red and green colors, respectively, were merged together digitally using the free software GIMP 2.6.7 (Free Software Foundation). Real-time videos were recorded using a digital consumer camcorder camera (HDR-SR7, Sony Electronics) connected to the microscope.

2.5 Cell culture and preparation of cell-laden alginate solution

Human embryonic kidney (HEK-293) cells were cultured in 5 % CO_2 at 37 °C in polystyrene tissue culture flasks. The used culture medium was DMEM containing 10 % FBS and 1 % antibiotics (penicillin/streptomycin). To prepare the cell-laden alginate solution, cells that reached 80–90 % confluency, were washed with PBS, and detached from the cell culture flask with 0.05 % trypsin-EDTA (1×) solution. Cells were suspended in the culture medium and counted in a Neubauer hemocytometer chamber (Bright-Line, Buffalo, NY). The cell suspension was centrifuged and the supernatant was discarded. Cells were re-suspended in 1:1 volumetric mixture of cell culture medium and sodium alginate 2 % (w/v), resulting in 1 % alginate solution. We used the cell density of 1×10^6 cells/ml in all experiments. The sheath flow solution was $CaCl_2$ 2 % (w/v) in 50 % glycerol in pH 7.0 HEPES buffer solution.

2.6 Cell viability test

Cell-laden fibers were kept in typical cell growth medium (DMEM supplemented with 10 % FBS and 1 % antibiotics) and placed in a 5 % CO2 incubator. Viability tests were performed by treating the fibers with LIVE/DEAD assay reagents (live/dead cell vitality assay kit (L34951) with C12 Resazurin & SYTOX® Green) according to the manufacturer's instructions. Using fluorescence microscopy, cell viability was examined by acquiring two images of each frame; red and green for live and dead cells, respectively. For testing the cell toxicity of chemicals used in the system, Trypan blue was used to determine the viability ratio of cells exposed to these chemicals. The procedure is discussed in details in the supplementary information.

3 Results and discussions

The fabricated MFDW head had multiple inputs and one output (Fig. 1). Inlets were connected to separate syringes containing cells suspended in sodium alginate, $CaCl_2$ for gelation and EDTA for declogging. The principle of fiber formation in the MFDW head is due to the coaxial microfluidic flow configuration, where a central stream of alginate is sheathed with a stream of $CaCl_2$ in the main channel, as demonstrated previously (Shin et al. 2007). Consequently, Ca^+ ions diffuse from $CaCl_2$ into the alginate central stream during the flow, forming calcium alginate cell-laden fibers before exiting the MFDW head (Fig. 1).

Typically, one MFDW was used repeatedly over a period of several months with no visible variation in the fibers being produced. Prior to each experiment, the MFDW was cleaned by soaking it in acetone and ethanol for 15 min.

Sodium alginate and $CaCl_2$ solutions were delivered using 1 ml Hamilton glass syringes. Alginate solution was injected through the vertical capillaries, whereas $CaCl_2$ solution was injected through the side capillary, see Fig. 1. At the junction, the $CaCl_2$ solution formed a sheath flow around the sodium alginate stream in a coaxial pattern and the calcium alginate gel was formed (Fig. 3a). The diameter of alginate fibers was characterized by changing the ratio of the flow rates of the alginate and the $CaCl_2$ solutions ($Q_{alginate}/Q_{CaCl2}$). Figure 3b illustrates a linear relationship between the ratio $Q_{alginate}/Q_{CaCl2}$ and the diameter of the formed fiber. If the dimensions of the MFDW head channels, the viscosity and the flow rate of the solutions are not properly selected; curling of fibers may occur (Fig. S2) (Shin et al. 2007). We noticed that using alginate stored for more than 2 months resulted in the formation of bulges in the fabricated fibers (Fig. S3). Therefore, we investigated the effects of various parameters such as flow rate and head geometry and optimized these variables to prevent fiber curling inside the MFDW head. Curling of the fiber was seen, when the outlet channel of the MFDW head was longer than 3 mm. The optimal length of the outlet channel was determined by direct writing of alginate with head lengths of 10 mm, 7 mm, 5 mm and 3 mm, where curling was seen in all of the lengths except for a 3 mm head length. The curling effect may also due to high upstream pressure of solutions flowing in the outlet channel. This pressure depends on the total flow rate of the sodium alginate and $CaCl_2$ as well as channel geometry (Akbari et al. 2009). For a MFDW head with a 3 mm long outlet channel, a total flow rate of <50 μl/min, and the ratio of sodium alginate to $CaCl_2$ flow rates in the range of 0.25–0.5 prevented the curling of the fibers.

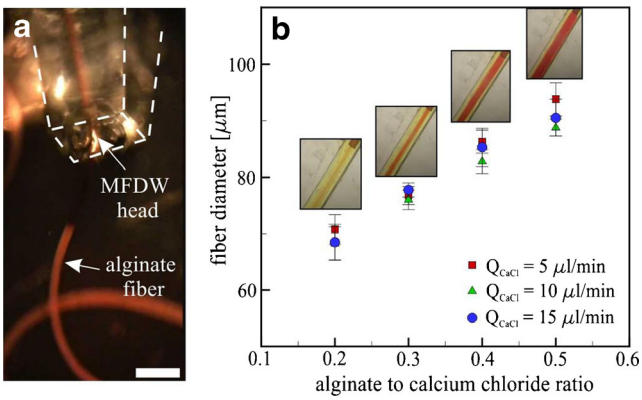

Fig. 3 Fiber extrusion and characterization of fiber size as a function of the flow rate ratio between alginate and $CaCl_2$ solutions. **a** Image of a fiber being extruded from the MFDW head's exit channel. Scale bar is 500 μm. **b** Characterization of the fiber diameter for three different $CaCl_2$ flow rates and four different flow rate ratios $Q_{alginate}/Q_{CaCl2}$. The workable range of ratios was between 0.2 and 0.5, and the fiber diameter ranged from ~70 to ~90 μm. The diameter of the alginate fiber is independent of the $CaCl_2$ flow rate, but increases linearly with the flow rate ratio

The difference between the sheath and core fluid viscosity combined with vibration caused by the movement of MFDW head resulted in flow instability during the writing process. To solve this challenge, we increased the viscosity of the sheath flow by adding 50 % (v/v) glycerol to the $CaCl_2$ solution. We also noticed that curling occurred when the speed of fiber exiting the MFDW was faster than the displacement speed of the tip (Fig. S2). On the other hand, if the fiber formation rate was lower than the speed of the MFDW tip stretching, pulling and dragging of the fiber was observed. Hence, the speed of fiber fabrication and of stage movement needs to be synchronized for reliable deposition of the fibers.

The ability of MFDW for depositing hydrogel fibers on a glass substrate under dry and immersed conditions was assessed. We reasoned that under immersed conditions the buoyancy force would help build larger 3D structures, while avoiding the collapse of the soft fiber scaffold. We noticed that the fibers do not attach to the surface of a non-treated glass. To promote the adhesion of the fibers to the substrate, we coated the substrate with aminosilane that is negatively charged at neutral pH and creates an electrostatic binding with positively charged alginate gel. With this approach, we enhanced fiber attachment to the substrate under the dry condition. However, in immersed condition, the adhesion of the fibers to the surface was insufficient to overcome the buoyancy force acting on the fibers.

Next, we tested the MFDW in air and found that the adhesion to the substrate was strong. The sheath flow kept the fibers humidified after delivery, which was important to keep the cells alive. The sheath solution also contains glycerol, which does not evaporate, is hygroscopic, and is used for cell storage, further contributing to ensuring cell survival. One of the challenges affecting the continuous scaffold fabrication process using the MFDW was the blockage of the outlet channel. This phenomenon was observed when the coaxial flow pattern was disturbed and calcium alginate fibers touched

the wall of the outlet channel and stuck to it. A key innovation in the MFDW presented here is the addition of a declogging mechanism for online restarting of the writing process upon channel blockage (see Section 2.3. Declogging mechanism). After the declogging of the MFDW head, the writing process could be resumed immediately. For this declogging mechanism to work efficiently, early injection of the EDTA was required, the longer the clogging had occurred the more difficult it was to remove the gel with this mechanism. For 1 % and 2 % (w/v) alginate crosslinked with 2 % $CaCl_2$, 30 mM of EDTA (with 0.15 M NaCl) in 1 mM HEPES buffer was used, however, for higher concentrations of calcium and alginate, higher concentrations of EDTA (and NaCl) was found to be more effective. Even thought this declogging mechanism adressed the clogging issue to a great extend, there were instances that large cloggings occurred which required the disassembly of the device. This occurred very rarely when a declogging was not flushed out immediately.

The shape of the fabricated constructs as well as the microstructure resolution and porosity were controlled by changing the diameter of the fibers and the flow rates of reagents. Figure 4 shows a typical alginate construct fabricated with the MFDW. To form this structure, several parallel lines were deposited on the surface in the x-direction (Fig. 4a), followed by a series of lines in the y-direction (Fig. 4b), and then in the x-direction, and so on. The MFDW head was moved up 100 μm prior to writing a new layer; this process is shown in Movie S1 in the Electronic supplementary information. The final grid structure formed in Fig. 4 is made of 1 % or 2 % alginate. Young's modulus for this alginate can range between 30 and 100 kPa (Steinbuchel 2009), which is in line with the extracellular matrix of soft tissues such as brain (Schiavone et al. 2009), liver and kidney (Opik et al. 2012), but this not sufficiently strong for making large scaffolds. More rigid structures could be built by increasing the alginate concentration, thus increasing the viscosity of the prepolymer, the calcium concentration to increase crosslinking as well as using higher G content alginates but the effects on cell viability will need to be assessed. For highly viscous solutions, it may be necessary to build the direct writer in rigid materials and use connections that can withhold higher pressures than is currently the case. Another option is to use mixture of alginate and other polymers such as collagen or chitosan that may also help increase the mechanical stability of the scaffold while at the same time enhancing cell proliferation (Sun and Tan 2013).

Next, we demonstrated the possibility of writing fibers loaded with cells on glass slides to form cell-laden constructs. Cells were detached from the cell culture dish, suspended in cell medium, and then mixed with the sodium alginate solution. The mixture was used with the MFDW to produce cell laden fibers. Figure 5 shows a calcium alginate structure in which HEK-293 cells are encapsulated. Cells at a concentration of 1×10^6 cells/ml in the alginate solution were used, however, this might be adjusted and optimized depending on the final application.

An important criterion for the success of this direct writing method is cell survival, which was confirmed by cell viability tests as outlined in the materials and methods. Alginate fibers containing HEK-293 cells were deposited into a 12-well cell culture plate containing cell medium using the MFDW. Fibers

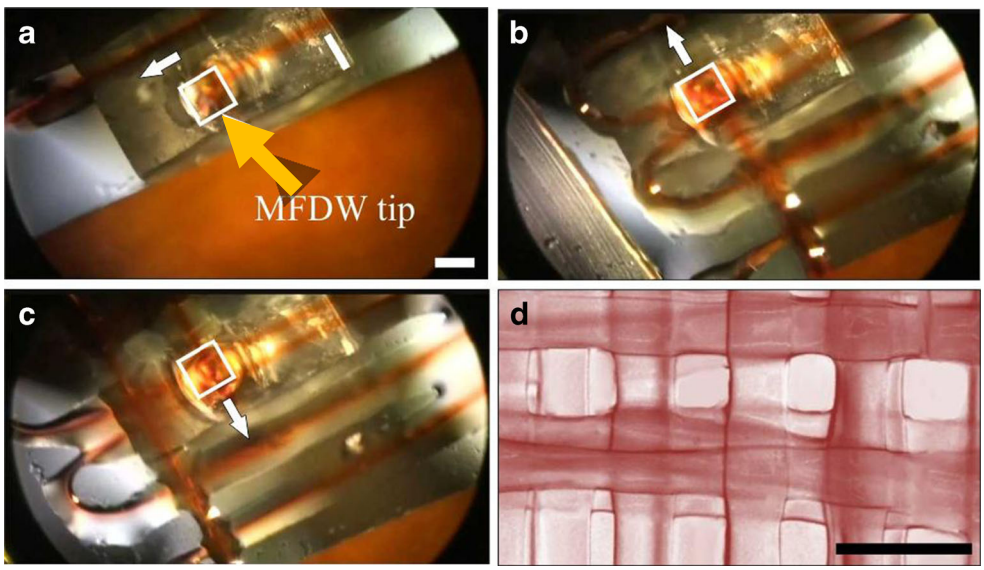

Fig. 4 Bottom view of direct writing of multiple layers of alginate fibers as grids on a glass slide. **a**–**c** Time-lapse images extracted from a real-time movie, captured during the writing of fibers. The tip of the MFDW head is highlighted with the *white box* and the *white arrows* indicate the direction of its movement as it leaves behind an alginate fiber to form the grid. The alginate is colored with red food dye, which appears orange here and the fibers are seen surrounded by the $CaCl_2$ solution (see Movie S1). Scale bar for (**a**)–(**c**) is 700 μm (**d**) The final multilayer construct with fibers of diameter of about 100 μm and spacing of approximately 100–150 μm patterned with the MFDW. Scale bars is 200 μm

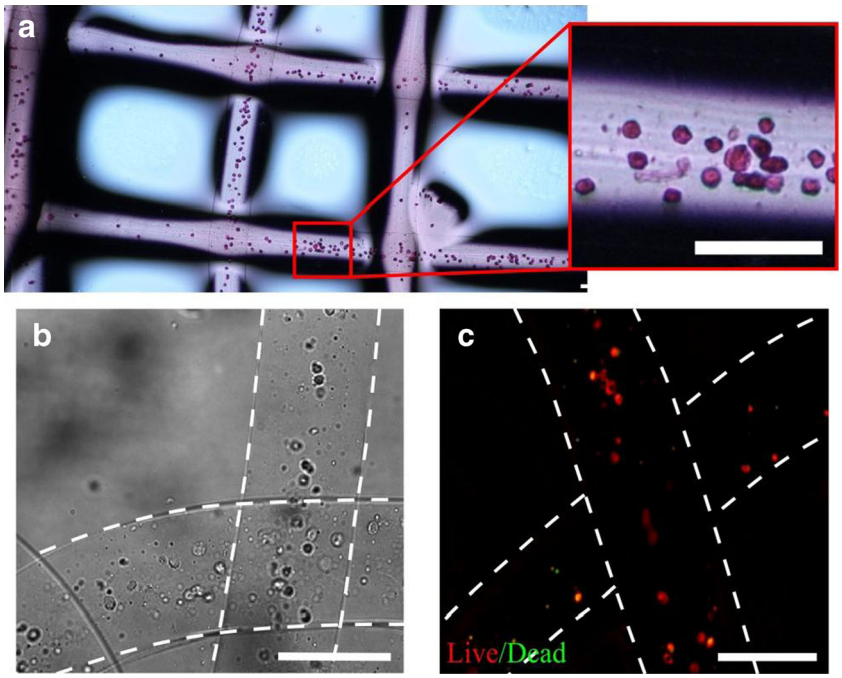

Fig. 5 HEK-293 cells encapsulated in alginate fibers deposited with the MFDW. **a** A grid was formed with the MFDW and stained with Trypan blue immediately after the process revealing many dead cells. However, following optimization of the buffer conditions HEK-293 cells shown in (**b**) Bright field (**c**) fluorescence (of another frame) were mostly alive and proliferating (live red, and green dead cells) and some are injured (*yellow*). Scale bars show 100 μm and *dashed lines* indicate the boundaries of the fibers

with HEK-293 cells were incubated in 5 % CO_2 at 37 °C and were examined for viability for a period of up to 3 days. Figure 5a shows cells after staining with Trypan blue revealing that most cells are dead. However, following optimization of the $CaCl_2$ solution and stabilization of the pH, Fig. 5b and c show that after 1 day only few cells were dead (green color), few cells were injured (yellowish), while the majority were healthy and alive (red color) cells confirming the biocompatibility of the writing process. Cell encapsulation in alginate fibers and incubation with optimized conditions showed 80± 3 % cell survival after 1 day of incubation and 89.5±2 % survival after 3 days of incubation in cell media within the fibers (data not shown). Figure 5c is a fluorescent image of cells incubated for 5 days, where red cells are live, and green cells are dead cells. The density of cells in these fibers has not yet been optimized and is lower than what it should be for tissue to form. It is worth noting that unmodified calcium alginate does not provide a nurturing environment for a variety of cell types. It will be interesting to use alginate functionalized with arginine–glycine–aspartate (RGD) motifs that promote cell adhesion and proliferation and observe the cell response (Rowley and Mooney 2002) and to examine critical factors such as proliferation and function of the cells in the gel.

The simultaneous writing of multiple hydrogels and cells can lead to the fabrication of more complex tissues. Such fabrication enables the placement of different cell types in predetermined locations of a scaffold towards replicating the microstructure of native tissues. To demonstrate the feasibility of the system to write constructs containing different cell types, we filled two syringes with two different colored alginate solutions and connected them to a T-junction (Fig. S1) that was then connected to the MFDW head; details are provided in the supplementary information. The syringe pumps were then synchronized to feed alternatively each of the alginate solution into the MFDW head at the desired location.

Figure 6 illustrates the deposition of alginate gel mixed with red dye (Fig. 6a) and the subsequent deposition of a layer of alginate mixed with a green dye (Fig. 6b). Switching of gels can be done on the fly, or while the MFDW is positioned outside of the writing area and moving back to writing mode to ensure that the new gel is delivered from a predetermined position. The process of switching gels is shown in Movie S1. Using additional flow splitters and syringe pumps loaded with different cell types, it should be possible to deliver a variety of different solutions. For example chitosan, poly(lactic-co-glycolic acid) (PLGA) (Hwang et al. 2008, 2009), and chitosan/alginate mixtures (Lee et al. 2011a) have been used to form hydrogel fibers and can also be used with the MFDW to produce scaffolds. The specific condition for the use of each material will need to be to be optimized. The MFDW is limited to low viscosity polymers, since the system works under low pressure and the injection of higher viscosity polymers require higher pressure.

4 Conclusions

We have introduced a MFDW for the fabrication of 3D cell-laden hydrogel constructs. The system allows for the “on the fly” formation of cell-containing fibers that are immediately deposited on a surface according to a predefined pattern using a computer program, while ensuring cell survival. Several

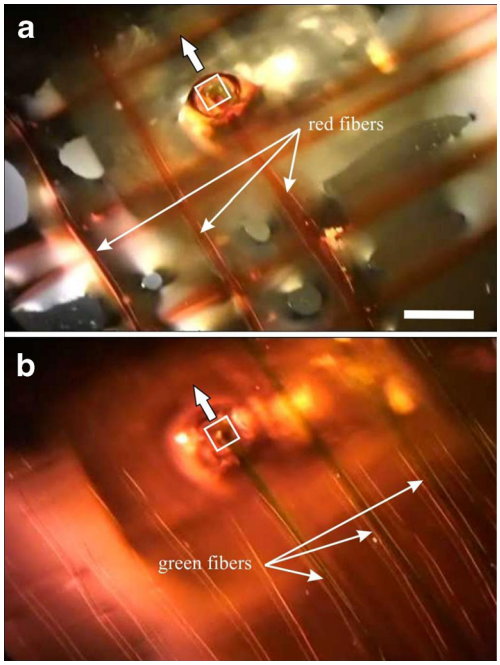

Fig. 6 Deposition of two different gels using the MFDW system. Three layers of red alginate fibers were first patterned on a substrate (**a**) followed by the deposition of a layer of green fibers, here seen as brownish (**b**) by switching between two syringe pumps. Scale bar shows 700 μm, the *white square* shows the tip of the MFDW, where the fiber exits and the *arrow* above it shows the direction of the movement of the MFDW. For the real time process refer to Movie S1

parameters, such as the shape and dimensions of the device, flow rate ratios, and the moving speed of the MFDW head were optimized. We observed that the moving speed of the MDFW head played an important role on the quality of the fabricated structure and should be synchronized with the fiber delivery rate. The maximum total flow rate of solutions through the MFDW head was 50 μl/min, while a ratio of sodium alginate to $CaCl_2$ flow rates between 0.25 and 0.5 μl/min produced straight fibers with diameters between 70 and 90 μm. A declogging feature with a channel containing a Ca^{2+} chelator (EDTA) was integrated and helped improving tolerance to clogging, which could be addressed on the fly, while direct writing could be resumed immediately, thus greatly enhancing the usability of the device. We demonstrated the fabrication of 3D structures through layer-by-layer deposition of cell-laden fibers in a predefined pattern, as well as of two different types of alginate fibers.

The main strength of the MFDW and other direct writing methods compared to molding systems is that the cells can be positioned in specific locations and interconnected networks of pores can be made within the construct. In comparison with other fiber-based techniques, such as electrospinning and wetspinning, direct writing has superior precision (Fedorovich et al. 2012). It should be noted that the developed MFDW is not limited to calcium alginate hydrogel, and other chemically, or optically cross-linkable hydrogels such as poly(lactic-co-glycolic acid), gelatin methacrylate, and polyvinyl alcohol may be used for creating cell-laden or cell-free constructs. We believe that the MFDW proposed here will help rapidly prototype more complex soft tissue scaffolds for use in research, and in the long term, for transplantation.

Acknowledgement We acknowledge funding from Natural Sciences and Engineering Research Council of Canada (NSERC), The Canadian Institutes of Health Research (CIHR), Certified Human Resources Professional (CHRP), Genome Canada, Genome Quebec, and Canada Foundation for Innovation (CFI.) M.A.Q. acknowledges Alexander Graham Bell Canada Graduate Scholarship (CGSD), M.A and A. T. acknowledge NSERC Postdoctoral fellowships, and D.J. acknowledges support from a Canada Research Chair. The authors thank Adiel Malik, Veronique Laforte, Sebastien Bergeron, and Kate Turner for critical reading of the manuscript.

References

M. Akbari, D. Sinton, M. Bahrami, Pressure drop in rectangular microchannels as compared with theory based on arbitrary cross section. J. Fluids Eng. **131**, 041202 (2009)

N. Annabi, A. Tamayol, J.A. Uquillas, M. Akbari, L. E. Bertassoni, C. Cha, G. Camci-Unal, M. R. Dokmeci, N. A. Peppas, A. Khademhosseini, 25th Anniversary Article: Rational design and applications of hydrogels in regenerative medicine. Advanced Materials. **26**, 85–124 (2014)

S. Arumuganathar, S. Irvine, J.R. McEwan, S.N. Jayasinghe, A novel direct aerodynamically assisted threading methodology for generating biologically viable microthreads encapsulating living primary cells. J. Appl. Polym. Sci. **107**(2), 1215–1225 (2008)

S.M. Berry, S.P. Warren, D.A. Hilgart, A.T. Schworer, S. Pabba, A.S. Gobin, R.W. Cohn, R.S. Keynton, Endothelial cell scaffolds generated by 3D direct writing of biodegradable polymer microfibers. Biomaterials **32**(7), 1872–1879 (2011)

E.J. Chung, M.J. Sugimoto, J. Koh, G. Ameer, Low pressure foaming: a novel method for the fabrication of porous scaffolds for tissue engineering. Tissue Eng. **18**(2), 113–121 (2011)

B.G. Chung, K.-H. Lee, A. Khademhosseini, S.-H. Lee, Microfluidic fabrication of microengineered hydrogels and their application in tissue engineering. Lab Chip **12**(1), 45–59 (2012)

V. Ellä, T. Annala, S. Länsman, M. Nurminen, M. Kellomäki, Knitted polylactide 96/4 L/D structures and scaffolds for tissue engineering. Biomatter **1**(1), 102–113 (2012)

N.E. Fedorovich, W. Schuurman, H.M. Wijnberg, H.-J. Prins, P.R. van Weeren, J. Malda, J. Alblas, W.J.A. Dhert, Biofabrication of osteochondral tissue equivalents by printing topologically defined, cell-laden hydrogel scaffolds. Tissue Eng. C **18**(1), 33–44 (2012)

R. Gaetani, P.A. Doevendans, C.H.G. Metz, J. Alblas, E. Messina, A. Giacomello, J.P.G. Sluijter, Cardiac tissue engineering using tissue printing technology and human cardiac progenitor cells. Biomaterials **33**(6), 1782–1790 (2012)

R. Gauvin, Y.C. Chen, J.W. Lee, P. Soman, P. Zorlutuna, J.W. Nichol, H. Bae, S. Chen, A. Khademhosseini, Microfabrication of complex porous tissue engineering scaffolds using 3D projection stereolithography. Biomaterials **33**(15), 3824–3834 (2012)

S. Ghorbanian, M.A. Qasaimeh, D. Juncker, Rapid prototyping of branched microfluidics in PDMS using capillaries. Chips and Tips (2010), http://blogs.rsc.org/chipsandtips/2010/05/03/rapid-prototyping-of-branched-microfluidics-in-pdms-using-capillaries/. Accessed 13 Feb 2014

L.D. Harris, B.-S. Kim, D.J. Mooney, Open pore biodegradable matrices formed with gas foaming. J. Biomed. Mater. Res. **42**(3), 396–402 (1998)

M.-H. Ho, P.-Y. Kuo, H.-J. Hsieh, T.-Y. Hsien, L.-T. Hou, J.-Y. Lai, D.-M. Wang, Preparation of porous scaffolds by using freeze-extraction and freeze-gelation methods. Biomaterials **25**(1), 129–138 (2004)

S.J. Hollister, Porous scaffold design for tissue engineering. Nat. Mater. **4**(7), 518–524 (2005)

C.M. Hwang, A. Khademhosseini, Y. Park, K. Sun, S.-H. Lee, Microfluidic chip-based fabrication of PLGA microfiber scaffolds for tissue engineering. Langmuir **24**(13), 6845–6851 (2008)

C. Hwang, Y. Park, J. Park, K. Lee, K. Sun, A. Khademhosseini, S. Lee, Controlled cellular orientation on PLGA microfibers with defined diameters. Biomed. Microdevices **11**(4), 739–746 (2009)

E. Kang, G.S. Jeong, Y.Y. Choi, K.H. Lee, A. Khademhosseini, S.-H. Lee, Digitally tunable physicochemical coding of material composition and topography in continuous microfibres. Nat. Mater. **10**, 877–883 (2011)

K. Katoh, T. Tanabe, K. Yamauchi, Novel approach to fabricate keratin sponge scaffolds with controlled pore size and porosity. Biomaterials **25**(18), 4255–4262 (2004)

G.H. Kim, S.H. Ahn, H.J. Lee, S.Y. Lee, Y. Cho, W. Chun, A new hybrid scaffold using rapid prototyping and electrohydrodynamic direct writing for bone tissue regeneration. J. Mater. Chem. **21**, 19138–19143 (2011)

R. Landers, A. Pfister, U. Hübner, H. John, R. Schmelzeisen, R. Mülhaupt, Fabrication of soft tissue engineering scaffolds by means of rapid prototyping techniques. J. Mater. Sci. **37**(15), 3107–3116 (2002)

B.R. Lee, K.H. Lee, E. Kang, D.-S. Kim, S.-H. Lee, Microfluidic wet spinning of chitosan-alginate microfibers and encapsulation of HepG2 cells in fibers. Biomicrofluidics **5**(2), 022208 (2011a)

G.-S. Lee, J.-H. Park, U.S. Shin, H.-W. Kim, Direct deposited porous scaffolds of calcium phosphate cement with alginate for drug delivery and bone tissue engineering. Acta Biomater. **7**(8), 3178–3186 (2011b)

L. Leng, A. McAllister, B. Zhang, M. Radisic, A. Günther, Mosaic hydrogels: one-step formation of multiscale soft materials. Adv. Mater. **24**(27), 3650–3658 (2012)

M.P. Lutolf, J.A. Hubbell, Synthetic biomaterials as instructive extracellular microenvironments for morphogenesis in tissue engineering. Nat. Biotechnol. **23**(1), 47–55 (2005)

S. Mazzitelli, L. Capretto, D. Carugo, X. Zhang, R. Piva, C. Nastruzzi, Optimised production of multifunctional microfibres by microfluidic chip technology for tissue engineering applications. Lab Chip **11**, 1776–1785 (2011)

G. Mazzoleni, D. Di Lorenzo, N. Steimberg, Modelling tissues in 3D: the next future of pharmaco-toxicology and food research? Genes Nutr. 4(1), 13–22 (2009)

L. Moroni, J.R. de Wijn, C.A. van Blitterswijk, Integrating novel technologies to fabricate smart scaffolds. J. Biomater. Sci. Polym. Ed. **19**(5), 543–572 (2008)

F.T. Moutos, L.E. Freed, F. Guilak, A biomimetic three-dimensional woven composite scaffold for functional tissue engineering of cartilage. Nat. Mater. **6**(2), 162–167 (2007)

Y.S. Nam, T.G. Park, Biodegradable polymeric microcellular foams by modified thermally induced phase separation method. Biomaterials **20**(19), 1783–1790 (1999)

S.C. Neves, L.S. Moreira Teixeira, L. Moroni, R.L. Reis, C.A. Van Blitterswijk, N.M. Alves, M. Karperien, J.F. Mano, Chitosan/Poly(ε-caprolactone) blend scaffolds for cartilage repair. Biomaterials **32**(4), 1068–1079 (2011)

C. Norotte, F.S. Marga, L.E. Niklason, G. Forgacs, Scaffold-free vascular tissue engineering using bioprinting. Biomaterials **30**(30), 5910–5917 (2009)

H. Onoe, T. Okitsu, A. Itou, M. Kato-Negishi, R. Gojo, D. Kiriya, K. Sato, S. Miura, S. Iwanaga, K. Kuribayashi-Shigetomi, Y. Shimoyama, Y.T. Matsunaga, S. Takeuchi, Metre-long cell-laden microfibres exhibit tissue morphologies and functions. Nat. Mater. **12**, 584–590 (2013)

R. Opik, A. Hunt, A. Ristolainen, P.M. Aubin, M. Kruusmaa, Development of high fidelity liver and kidney phantom organs for use with robotic surgical systems Biomedical Robotics and Biomechatronics (BioRob), 2012 4th IEEE RAS & EMBS International Conference on (2012), pp. 425–430

F. Pampaloni, E.G. Reynaud, E.H.K. Stelzer, The third dimension bridges the gap between cell culture and live tissue. Nat. Rev. Mol. Cell Biol. **8**(10), 839–845 (2007)

J.S. Park, D.G. Woo, B.K. Sun, H.-M. Chung, S.J. Im, Y.M. Choi, K. Park, K.M. Huh, K.-H. Park, In vitro and in vivo test of PEG/PCL-based hydrogel scaffold for cell delivery application. J. Control. Release **124**(1–2), 51–59 (2007)

C.M. Perrault, M.A. Qasaimeh, T. Brastaviceanu, K. Anderson, Y. Kabakibo, D. Juncker, Rev. Sci. Instrum. **81**(11), 115107–115108 (2010)

J.A. Rowley, D.J. Mooney, Alginate type and RGD density control myoblast phenotype. J. Biomed. Mater. Res. **60**(2), 217–223 (2002)

P. Schiavone, F. Chassat, T. Boudou, E. Promayon, F. Valdivia, Y. Payan, In vivo measurement of human brain elasticity using a light aspiration device. Med. Image Anal. **13**(4), 673–678 (2009)

Z. Shi, N. Chen, Y. Du, A. Khademhosseini, M. Alber, Stochastic model of self-assembly of cell-laden hydrogels. Phys. Rev. E **80**(6), 061901 (2009)

S.-J. Shin, J.-Y. Park, J.-Y. Lee, H. Park, Y.-D. Park, K.-B. Lee, C.-M. Whang, S.-H. Lee, "On the fly" continuous generation of alginate fibers using a microfluidic device. Langmuir **23**(17), 9104–9108 (2007)

A. Steinbuchel, *Alginates: Biology and Applications* (Springer, Germany, 2009)

J. Sun, H. Tan, Alginate-based biomaterials for regenerative medicine applications. Materials **6**(4), 1285–1309 (2013)

A. Tamayol, M. Akbari, N. Annabi, A. Paul, A. Khademhosseini, D. Juncker, Fiber-based tissue engineering: Progress, challenges, and opportunities. Biotechnology Advances **31**(5), 669–687 (2013)

K.H. Tan, C.K. Chua, K.F. Leong, C.M. Cheah, W.S. Gui, W.S. Tan, F.E. Wiria, Selective laser sintering of biocompatible polymers for applications in tissue engineering. Biomed. Mater. Eng. **15**(1), 113–124 (2005)

L. Vogelaar, J.N. Barsema, C.J.M. van Rijn, W. Nijdam, M. Wessling, Phase separation micromolding—PSμM. Adv. Mater. **15**(16), 1385–1389 (2003)

X. Wang, W. Li, V. Kumar, A method for solvent-free fabrication of porous polymer using solid-state foaming and ultrasound for tissue engineering applications. Biomaterials **27**(9), 1924–1929 (2006)

F.E. Wiria, K.F. Leong, C.K. Chua, Y. Liu, Poly-ε-caprolactone/hydroxyapatite for tissue engineering scaffold fabrication via selective laser sintering. Acta Biomater. **3**(1), 1–12 (2007)

K.M. Yamada, E. Cukierman, Modeling tissue morphogenesis and cancer in 3D. Cell **130**(4), 601–610 (2007)

M. Yamada, S. Sugaya, Y. Naganuma, M. Seki, Microfluidic synthesis of chemically and physically anisotropic hydrogel microfibers for guided cell growth and networking. Soft Matter **8**, 3122–3130 (2012)

Y. Yokoyama, S. Hattori, C. Yoshikawa, Y. Yasuda, H. Koyama, T. Takato, H. Kobayashi, Novel wet electrospinning system for fabrication of spongiform nanofiber 3-dimensional fabric. Mater. Lett. **63**(9–10), 754–756 (2009)

Microfluidic Direct Writer for Fabricating Cell-Laden Hydrogel Constructs

Setareh Ghorbanian, Mohammad A. Qasaimeh, Mohsen Akbari,

Ali Tamayol, and David Juncker

Supplementary Material

S1. Connecting more than one alginate streams to the microfluidic direct writer

A small piece (3 cm long) of glass capillary (ID 180 μm, OD 360 μm) was pulled to form a tip, with an inner diameter of approximately 100 μm, or a pointed capillary was prepared by inserting a smaller capillary (ID 100 μm, OD 180 μm) into the larger one (ID 180 μm, OD 360 μm). This capillary was then connected to a single-channel sleeve and then to a double-channel sleeve holding two longer capillaries (30 cm) using Upchurch scientific fittings (Fig. S1). The double-hole sleeve was connected to two different glass capillaries connected to two separate syringes each containing a different alginate solution.

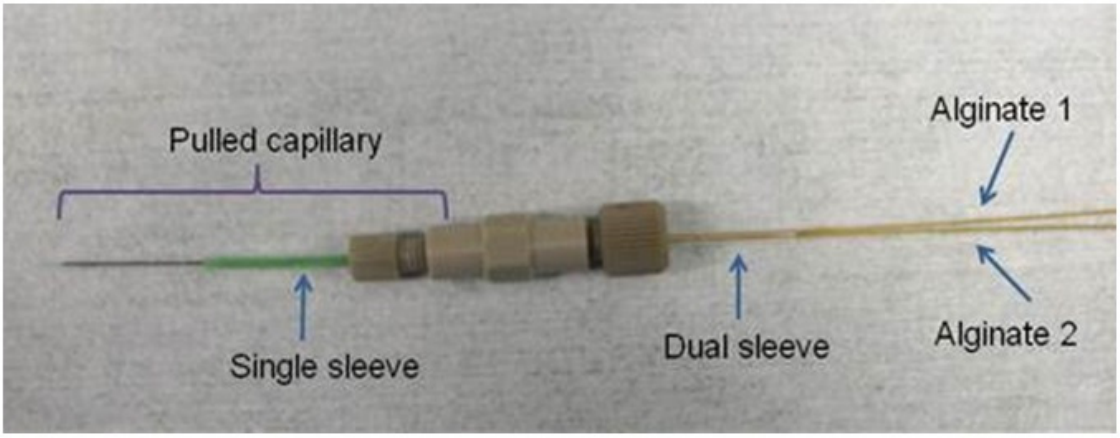

Fig.S1 T-connection, connecting two syringes with different cells to a pulled capillary or one with the smaller inserted tip.

S2. Cell toxicity experiments for all reagents

HEK cells were cultured in 12 well plates. After two days of incubation in cell medium, the media was removed and replaced with 500 µl of the following: 2% $CaCl_2$, 2% $CaCl_2$ in (50%, 25% or 10%) glycerol, 2% $CaCl_2$ in HEPES buffer and 50% glycerol, 0.5% EDTA or red, green or blue food dyes. Cells were incubated with the above mentioned solutions for 30 minutes. Solutions were then removed, and replaced with 0.5 ml trypsin and EDTA mixture for 30 minutes. Subsequently 0.5 ml cell media was added and the content of the wells were placed into centrifuge tubes where 0.2 ml Trypan blue was added, incubated for 15 minutes and counted for live/dead cell number.

To examine the effect of encapsulation and direct writing of cells within alginate fibers, biocompatibility and toxicity tests were done. When treated with EDTA, most cells were already detached during incubation; therefore, cell number was very low. However, cells which were still attached to the surface (10% of the original number) were 80% live. When treated with $CaCl_2$,

50% cell death was observed. When glycerol was added to the solutions, 75% cell death was observed for all percentages of glycerol due to the acidic effect. However, when incubated with 2% $CaCl_2$ with 50% glycerol in HEPES of pH7, 99% cells were attached and alive.

S3. Fiber curling and bulging

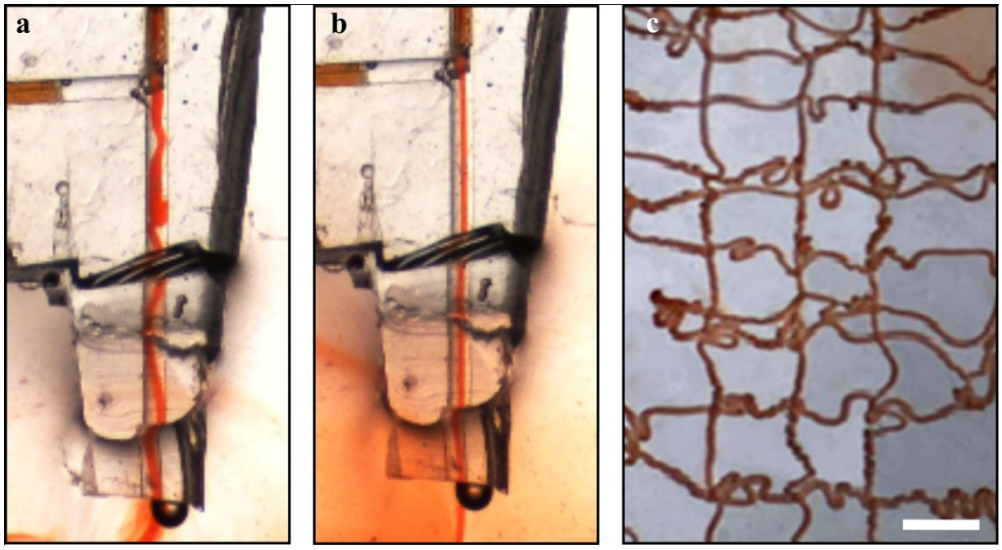

Fig.S2 Formation of curls during the direct write of alginate fibers.(a) Instability of the alginate stream and fiber curling inside the MFDW head due to high $Q_{alginate}/Q_{CaCl2}$ (0.7 here) that could cause channel blockage. (b) Stable coaxial flow by lowering $Q_{alginate}/Q_{CaCl2}$ (0.4 here) in the same MFDW head that prevents fiber curling. (c) Curling of direct written fibers outside the MFDW head, which are results of a high fiber delivery rate and a lower MFDW writing speed.

Fig.S3 Bulges observed on alginate fibers delivered into a bath. The fibers contained 0.5 μm diameter fluorescent beads. Bulging occurred when alginate solution was prepared more than two months before experiments. Hence for further experiments, alginate was always kept and used for maximum of two months. Scale bar is presenting 200 μm.